Am J Physiol Endocrinol Metab 284: E1089–E1097, 2003.
First published February 11, 2003; 10.1152/ajpendo.00540.2002.

Differential activation of NF-κB and AP-1 in increased fibronectin synthesis in target organs of diabetic complications

Shali Chen, Zia Ali Khan, Mark Cukiernik, and Subrata Chakrabarti
Department of Pathology, University of Western Ontario, London, Ontario N6A 5C1, Canada

Submitted 11 December 2002; accepted in final form 3 February 2003

Chen, Shali, Zia Ali Khan, Mark Cukiernik, and Subrata Chakrabarti. Differential activation of NF-κB and AP-1 in increased fibronectin synthesis in target organs of diabetic complications. *Am J Physiol Endocrinol Metab* 284: E1089–E1097, 2003. First published February 11, 2003; 10.1152/ajpendo.00540.2002.—Increased extracellular matrix protein production leading to structural abnormalities is a characteristic feature of chronic diabetic complications. We previously showed that high glucose in endothelial cell culture leads to the upregulation of basement membrane protein fibronectin (FN) via an endothelin (ET)-dependent pathway involving activation of NF-κB and activating protein-1 (AP-1). To delineate the mechanisms of basement membrane thickening, we used an animal model of chronic diabetes and evaluated ET-dependent activation of NF-κB and AP-1 and subsequent upregulation of FN in three target organs of chronic diabetic complications. After 3 mo of diabetes, retina, renal cortex, and myocardium demonstrated increased FN mRNA and increased ET-1 mRNA expression. Increased FN expression was shown to be dependent on ET receptor-mediated signaling, as the increase was prevented by the dual ET receptor antagonist bosentan. NF-κB activation was most pronounced in the retina, followed by kidney and heart. AP-1 activation was also most pronounced in the retina but was similar in both kidney and heart. Bosentan treatment prevented NF-κB activation in the retina and heart and AP-1 activation in the retina and kidney. These data indicate that, although ETs are important in increased FN production due to diabetes, the mechanisms with respect to transcription factor activation may vary depending on the microenvironment of the organ.

activating protein-1; nuclear factor-κB; endothelin; retina; kidney; heart; diabetes

CAPILLARY BASEMENT MEMBRANE (BM) THICKENING is a hallmark of diabetic microangiopathy and has been demonstrated in all target organs of diabetic complications, including retina, kidney, and heart (4, 21). Although the mechanism is not clear, various biochemical pathways have been associated with capillary BM thickening due to diabetes (2, 4, 5, 21). At the molecular level, increased extracellular matrix (ECM) protein synthesis is instrumental in BM thickening (8, 15, 36). Fibronectin (FN), a glycoprotein of ~250 kDa, is a major component of the ECM. It is composed of two similar, but not identical, polypeptides joined by disulfide bonds. FN plays key roles in various cellular events, including cell adhesion, motility, and tissue repair (3, 22, 41). However, its overproduction may decrease the motility and replication of many cells, including endothelial cells (28). Physiologically, upregulation of FN may lead to increased retinal vascular endothelial cell turnover due to diabetes (29). FN synthesis has been demonstrated to increase in the retina of diabetic patients with background retinopathy (36). Several factors may influence augmented FN synthesis in diabetes. Vasoactive factors like endothelins (ETs), by virtue of their extensive tissue distribution and widespread biological actions, are important mediators of pathogenic changes in diabetic microangiopathy and may influence FN production (8, 9, 15). We have previously demonstrated (8, 12, 15) that ET-1 and ET-3 expressions are upregulated in the retina of diabetic rats and that ET receptor blockade prevents hyperhexosemia-induced vasoconstriction and BM thickening in the retina and glomeruli of diabetic rats. We have also shown (9) that diabetes-induced myocardial focal scarring can be prevented by ET antagonism. Several biochemical pathways, such as protein kinase C (PKC) activation, nonenzymatic glycation, and activation of other vasoactive factors, may promote increased ET synthesis and subsequent FN increase (2, 4, 7, 21, 27). ETs have been shown to produce fibrosis via activation of transcription factors NF-κB and activating protein (AP)-1. ET-1 activates NF-κB in the hepatic stellate cells via the ET_B receptor (16). Angiotensin II-induced end organ damage in hypertension has been shown to be mediated via ET receptor-dependent NF-κB and AP-1 activation (31). Various pathways of tissue injury caused by hyperglycemia in vivo or high glucose concentration in cell cultures may activate transcription factors such as NF-κB and AP-1 and subsequently alter the expression of several genes important in the pathogenesis of diabetic complications (30, 32, 33). NF-κB is present in several cell types, including endothelial cells (39). Normally, inactive NF-κB exists in the cytoplasm, bound to the inhibitory protein IκB. IκB is hydrolyzed following stimulation, whereby the p50/p65 dimer translocates to the nucleus and initiates transcription of various genes (1, 6, 17, 30, 32). Resynthesis of IκB, induced by NF-κB, allows sequestration of NF-κB in

Address for reprint requests and other correspondence: S. Chakrabarti, Dept. of Pathology, Dental Sciences Bldg, Univ. of Western Ontario, London, ON N6A 5C1, Canada (E-mail: schakrab@uwo.ca).

The costs of publication of this article were defrayed in part by the payment of page charges. The article must therefore be hereby marked "*advertisement*" in accordance with 18 U.S.C. Section 1734 solely to indicate this fact.

Table 1. *Primer sequences and temperature profiles for RT-PCR*

Primer Sequences	PCR Parameters, temperature-time/ramp rate		Melting-Curve Analysis, temperature-time/ramp rate	
Fibronectin	Denaturation	95°C-0s 20°C/s	Step 1	95°C-0s 20°C/s
5′-CCAGGCACTGACTACAAGAT-3′ 5′-CATGATACCAGCAAGGACTT-3′				
	Annealing	60°C-5s 20°C/s	Step 2	70°C-15s 20°C/s
	Extension	72°C-17s 20°C/s	Step 3	95°C-0s 0.10°C/s
	Signal	84°C-1s 20°C/s	Signal	continuous
Endothelin-1	Denaturation	95°C-0s 20°C/s	Step 1	95°C-0s 20°C/s
5′-GCTCCTGCTCCTCCTTGATG-3′ 5′-CTCGCTCTATGTAAGTCATGG-3′				
	Annealing	58°C-5s 20°C/s	Step 2	63°C-15s 20°C/s
	Extension	72°C-20s 20°C/s	Step 3	95°C-0s 0.10°C/s
	Signal	84°C-1s 20°C/s	Signal	continuous
β-Actin	Denaturation	95°C-0s 20°C/s	Step 1	95°C-0s 20°C/s
5′-CCTCTATGCCAACACAGTGC-3′ 5′-CATCGTACTCCTGCTTGCTG-3′				
	Annealing	58°C-5s 20°C/s	Step 2	67°C-15s 20°C/s
	Extension	72°C-8s 20°C/s	Step 3	95°C-0s 0.10°C/s
	Signal	83°C-1s 20°C/s	Signal	continuous

the cytoplasm and termination of NF-κB response (1, 6, 17). AP-1 consists of homodimers of Jun or heterodimers of Fos and Jun (11, 38). It is also regulated by cellular stress. Coordinated participation of NF-κB and another transcription factor such as AP-1 may activate the genes of the effector molecules in various pathological conditions (11, 38). We have previously demonstrated (10) that endothelial cells cultured in 25 mmol/l glucose upregulate the expression of FN, thus mimicking the effects of diabetes. We have further demonstrated that, in endothelial cells, such glucose-induced increased FN expression is mediated via ET through activation of both NF-κB and AP-1 (10). The aim of the present study was to determine the role of NF-κB and AP-1 in increased FN mRNA expression in the various clinically relevant target organs of diabetic complications. We further investigated whether these changes are dependent on ET alteration.

MATERIALS AND METHODS

Reagents. All reagents were obtained from Sigma Chemical (St. Louis, MO) unless otherwise mentioned.

Animals. All animals were cared for in accordance with the Declaration of Helsinki and the Guiding Principles in the Care and Use of Animals. The University of Western Ontario Council on Animal Care Committee formally approved all experimental protocols. Male Sprague-Dawley rats of ~200 g were obtained from Charles River Canada (St. Constant, PQ, Canada). Diabetes was induced with a single intravenous injection of streptozotocin (65 mg/kg body wt, in citrate buffer). The presence of hyperglycemia was confirmed by blood glucose estimation (Surestep blood glucose meter; Lifescan, Burnaby, BC, Canada). Nondiabetic control animals received an equal-volume injection of citrate buffer. Diabetic rats were randomized into two groups, namely, *1*) poorly controlled diabetics and *2*) poorly controlled diabetics on bosentan treatment. Age- and sex-matched animals were used as nondiabetic controls.

Bosentan (courtesy of Dr. M. Clozel, Actelion, Basel, Switzerland) is a potent dual ET_A and ET_B receptor antagonist (35). Bosentan was administered by daily oral gavage at the dose of 100 mg·kg body wt^{-1}·day^{-1} (12, 15). Treatment started at the onset of diabetes and continued daily for the follow-up period. The animals were housed in individual, air-filtered metabolic cages, given rat chow and water ad libitum, and monitored daily for glucosuria and ketonuria (Uriscan Gluketo, Yeong Dong, Seoul, Korea). Diabetic animals received small daily doses (0.1–3.0 U) of Ultralente insulin (Novo Nordisk, Princeton, NJ) to maintain hyperglycemia between 15 and 25 mmol/l and to prevent ketoacidosis. Systolic blood pressure was recorded by tail plethysmography before animals were killed (23). Blood, urine, and tissues were collected from seven randomly selected animals from each group after 3 mo of follow-up for glycated hemoglobin measurement (Sigma), urine albumin mea-

Table 2. *Oligonucleotide sequences for EMSA*

Transcription Factor	Consensus Oligonucleotide Sequences
NF-κB	5′-AGTTGAGGGGACTTTCCCAGGC-3′ 3′-TCAACTCCCCTGAAAGGGTCCG-5′
AP-1	5′-CGCTTGATGAGTCAGCCGGAA-3′ 3′-GCGAACTACTCAGTCGGCCTT-5′

EMSA, electrophoretic mobility shift assay; AP-1, activating protein-1.

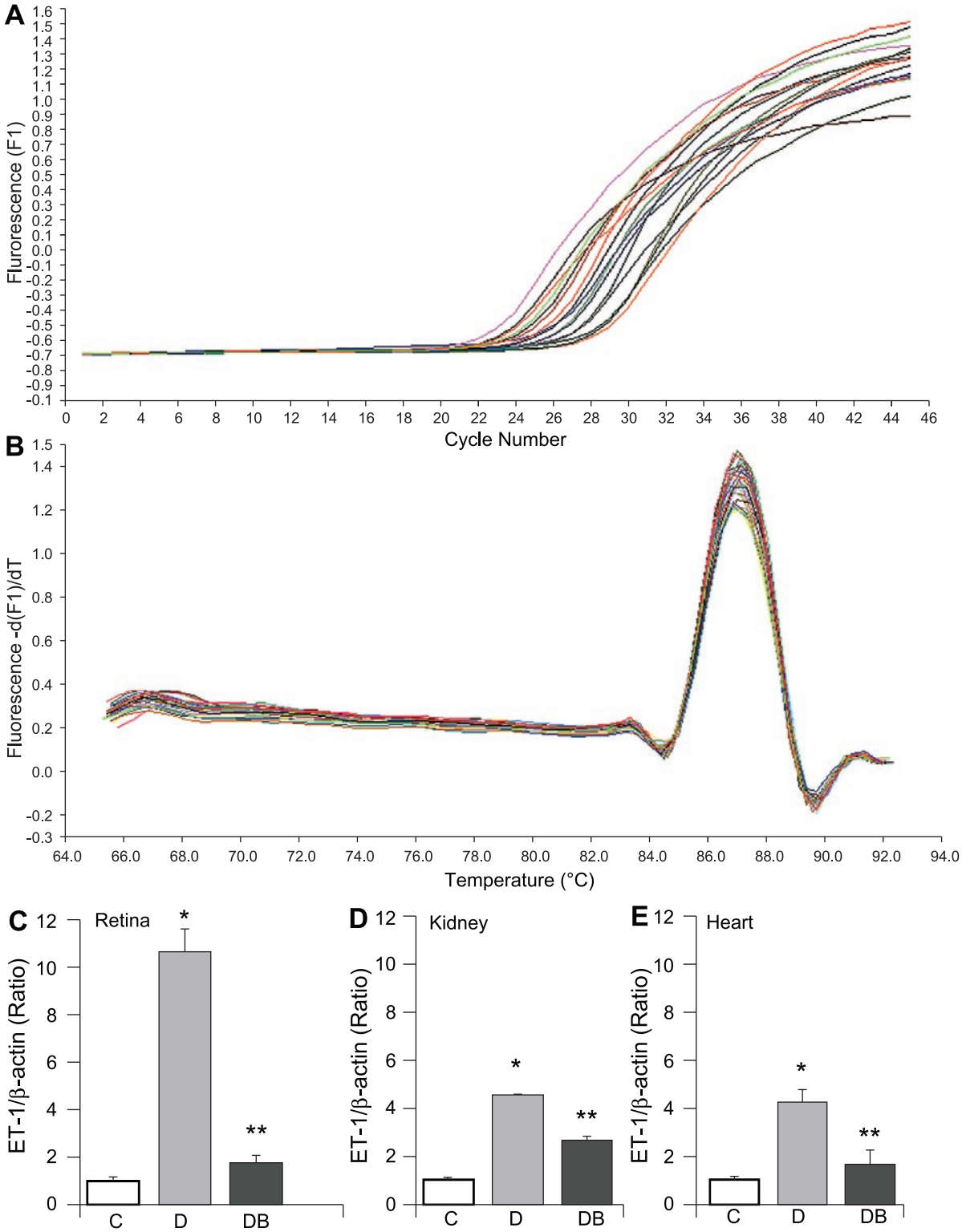

Fig. 1. Endothelin (ET)-1 mRNA quantification in rat tissues by real-time RT-PCR. *A*: PCR amplification plot of ET-1. ET-1 mRNA was subjected to real-time RT-PCR. Crossing point (C_p) value, obtained from SYBR Green I signal, was used to compute relative concentration of ET-1 mRNA from ET standard curve. *B*: PCR products were also subjected to melting-curve analysis to determine specificity of the products. All samples showed a specific product, with melting temperature (T_m) of 87°C. *C–E*: ET-1 mRNA normalized to β-actin. *C-E*: ET-1 mRNA levels (means ± SE) in the retina (*C*), kidney (*D*), and heart (*E*) of the nondiabetic controls (C), poorly controlled diabetics (D), and bosentan-treated diabetics (DB) as measured by real-time RT-PCR. *Significantly different from C; **significantly different from D; $n = 6$ in each group.

surement (Nephrat kit; Exocell Philadelphia, PA), and other analyses. All investigations listed below were performed in a masked fashion.

The animals were killed after 3 mo of treatment. Tissues obtained from the rats were divided into portions. Some portions were immediately used for nuclear protein extraction, and the remaining tissues were snap-frozen in liquid nitrogen for RNA extraction and gene expression analysis.

Preparation of nuclear protein fractions. Nuclear extracts of kidney, heart, and retina were prepared as described elsewhere (13, 37). Rapid detection of octamer-binding proteins with "miniextracts" was prepared from a small amount of tissue (0.5–1 g) as previously described (10, 37). Briefly, the tissues were homogenized, washed with phosphate-buffered saline, and pelleted by centrifugation (1,500 *g* for 5 min). The pellet was resuspended in 0.4 ml of cold *buffer A* (in mmol/l: 10 HEPES, pH 7.9, 10 KCl, 0.1 EDTA, 0.1 EGTA, 1 DTT, and 0.5 PMSF) by gentle pipetting. The cells were allowed to swell on ice for 15 min. Twenty-five microliters of 10% IGEPAL CA-630 were added, and cells were vortexed vigorously. The homogenate was centrifuged (10,000 *g* for 30 s), and the nuclear pellet was resuspended in 50 μl of ice-cold *buffer C* (in mmol/l: 20 HEPES, pH 7.9, 0.4 NaCl, 1 EDTA, 1 EGTA, 1 DTT, and 1 PMSF). The tube was vigorously rocked at 4°C for 15 min on a shaking platform. The nuclear extract was centrifuged at 4°C (15,000 *g* for 5 min), and the supernatant was frozen at −70°C. The protein concentrations were measured using the bicinchoninic acid protein assay, with bovine serum albumin as a standard (Pierce, Rockford, IL).

Electrophoretic mobility shift assay. Electrophoretic mobility shift assays (EMSA) were performed following established methodology and as described by us previously (10). Briefly, NF-κB and AP-1 consensus oligonucleotide (Promega, WI) DNA probes (Table 2) were prepared by end labeling with [γ-^{32}P]ATP (Amersham, QC, Canada) using T4 polynucleotide kinase. The probes were purified by ethanol precipitation and resuspended in 10 mmol/l Tris and 1 mmol/l EDTA (pH 7.6). Five micrograms of nuclear proteins were incubated with 100,000 cpm of ^{32}P-labeled consensus oligonucleotides for 30 min at room temperature. The incubation was carried out in a buffer containing 10 mmol/l Tris (pH 7.5), 50 mmol/l NaCl, 1 mmol/l $MgCl_2$, 5% glycerol, 0.05% IGEPAL CA-630, 0.5 mmol/l EDTA, 0.5 mmol/l DTT, and 0.5 μg of poly(dI-dC). Protein-DNA complexes were resolved on a standard 6% (NF-κB) and 4% (AP-1) nondenaturing polyacrylamide gel in 0.5 × Tris-boric acid-EDTA running buffer. After 30 min of electrophoresis at 350 V, gels were dried under heated vacuum onto Whatman paper and subjected to autoradiography from overnight to 3 days. Anti-NF-κB (p65) monoclonal antibody and anti-AP-1 (c-Jun) polyclonal antibody (Santa Cruz Biotechnology, Santa Cruz, CA) were used for the supershift assay. The specificity of binding was further confirmed by incubation with 100-fold unlabeled oligonucleotides. The blots were quantified with densitometry (10).

RNA isolation. TRIzol reagent (Invitrogen, Burlington, ON, Canada) was used to isolate RNA. RNA was extracted with chloroform followed by centrifugation to separate into aqueous and organic phases. RNA was recovered from the aqueous phase by isopropyl alcohol precipitation and suspended in diethylpyrocarbonate-treated water (8, 15).

First-strand cDNA synthesis. First-strand cDNA synthesis was performed using the Superscript-II system (Invitrogen). RNA (3 μg) was added to oligo(dT) primers (Invitrogen), denatured at 65°C, and quenched on ice for 10 min. Reverse transcription was carried out by the addition of Moloney murine leukemia virus reverse transcriptase and dNTP at 42°C for 50 min in a total reaction volume of 20 μl. The reaction was terminated by incubation at 70°C for 15 min. The resulting RT products were stored at −20°C (8, 15).

Real-time RT-PCR. RT-PCR was carried out with the LightCycler (Roche Diagnostics Canada, Laval, PQ, Canada) using the SYBR Green I detection platform. This system allows amplification and detection of products in a single reaction tube. PCR reactions were performed in microcapillary tubes (Roche Diagnostics Canada), with a final volume of 20 μl. The reaction mixture consisted of 2.5 μl of 10 × PCR buffer (Invitrogen), 1.25 μl of 5 mM dNTP, 1.2 μl of 50 mM $MgCl_2$ (1.6 μl for ET-1), 1 μl each of forward and reverse 10 μM primers, 0.5 μl of 5 U/μl Platinum Taq polymerase, 0.75 μl of 10 × SYBR Green I (Molecular Probes, Eugene, OR), 10.8 μl of H_2O, and 1 μl of cDNA template.

The temperature profiles and primer sequences for PCR reactions are found in Table 1. To optimize the amplification of the genes, melting curve analysis (MCA) was used to determine the melting temperature (T_m) of specific products and primer dimers. According to the T_m value of specific products for respective genes, an additional step (signal acquisition step, 2–3°C below T_m) was added after the elongation phase of RT-PCR. This additional step in the PCR reactions allowed for signal acquisition from specific target products. The signal acquisition step was determined to be 83°C for β-actin and 84°C for FN and ET-1.

FN and ET-1 mRNA was quantified with the standard curve method. Standard curves for all genes were constructed using different amounts of standard template. The cycle number, crossing point (C_p), which produces a significantly different fluorescence signal from baseline, was used to compute the relative concentration of target genes from the standard curves. The data were normalized to β-actin to account for differences in reverse transcription efficiencies and the amount of template in each reaction mixture.

Statistical analysis. The data are expressed as means ± SE and were analyzed by ANOVA followed by Student's *t*-test. Differences were considered significant at values of $P < 0.05$.

RESULTS

Clinical monitoring. Poorly controlled diabetic animals demonstrated hyperglycemia (19.0 ± 2.5 vs. 4.6 ± 0.2 mmol/l in controls), reduced body weight gain (482 ± 18.2 vs. 627 ± 21.7 g), and increased glycated hemoglobin levels (17.4 ± 0.6 vs. 5.6 ± 0.4% in controls) compared with the age-matched nondiabetic con-

Fig. 2. Fibronectin (FN) mRNA quantification in rat tissues by real-time RT-PCR. *A*: PCR amplification plot of FN. FN mRNA was subjected to real-time RT-PCR. C_p value obtained from SYBR Green I signal was used to compute relative concentration of FN mRNA from FN standard curve. *B*: PCR products were also subjected to melting-curve analysis to determine specificity of the products. All samples showed a specific product, with T_m of 87°C. Lower panel represents FN mRNA normalized to β-actin. *C–E*: FN mRNA levels (means ± SE) in the retina (*C*), kidney (*D*), and heart (*E*) of the nondiabetic controls (C), poorly controlled diabetics (D), and bosentan-treated diabetics (DB) as measured by real-time RT-PCR. *Significantly different from C; **significantly different from D; $n = 6$ in each group.

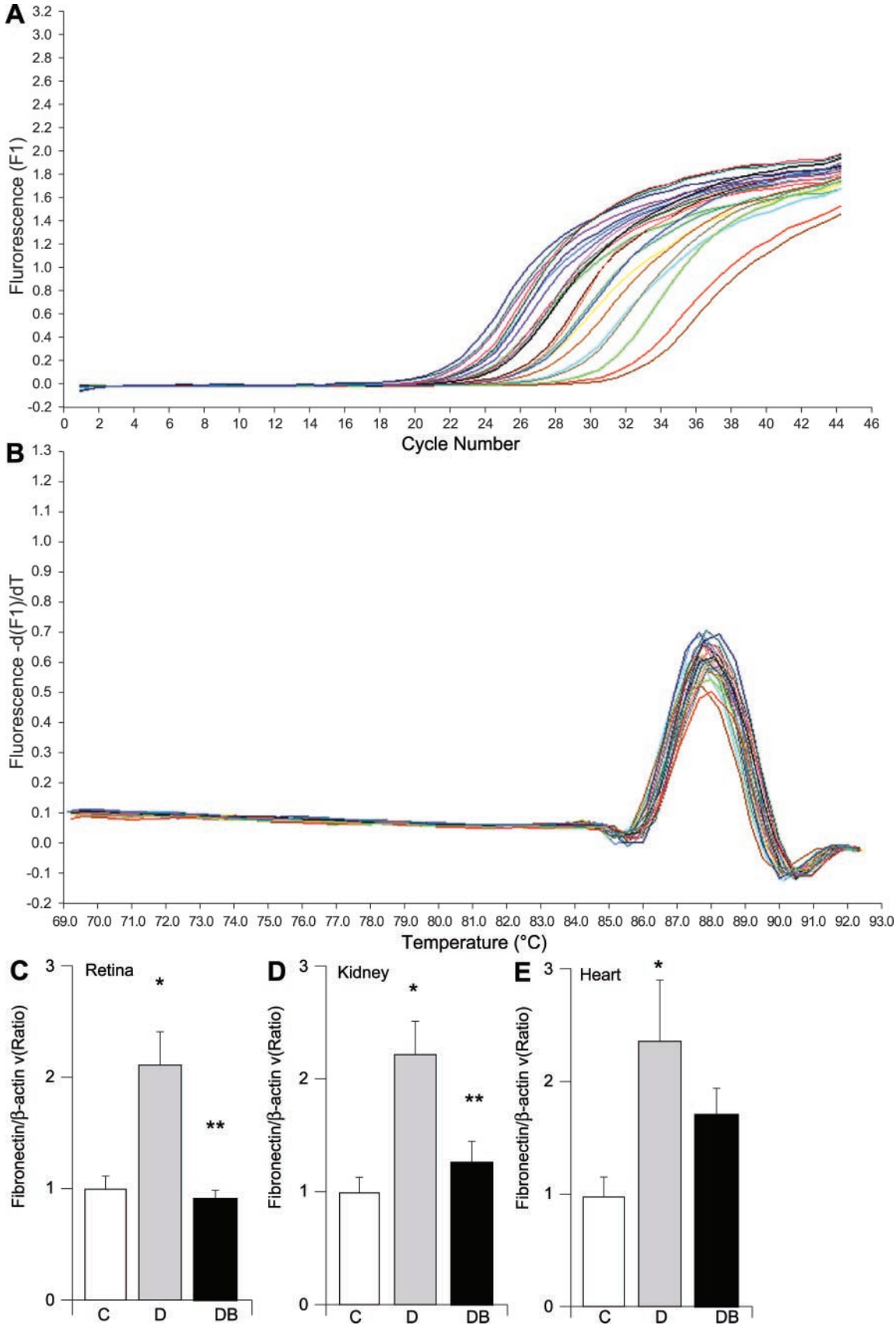
A
Flurorescence (F1)
Cycle Number
B
Fluorescence -d(F1)/dT
Temperature (°C)
C
Retina
D
Kidney
E
Heart
Fibronectin/β-actin v(Ratio)
C
D
DB
*
**

trol animals. These rats also demonstrated polyuria and glucosuria (data not shown). These data are indicative of diabetic dysmetabolism. Bosentan treatment had no effects on these parameters (20.7 ± 1.6 mmol/l, 489 ± 12.7 g, and 15.8 ± 0.5%, respectively). No alterations of blood pressure were seen in any of the groups.

Diabetes-induced ET-1 mRNA upregulation. We have previously demonstrated (8, 9, 12, 15) that chronic diabetes induces ET-1 mRNA upregulation in retina, kidney, and heart. This study confirmed our previous finding that ET-1 mRNA upregulation occurs in all target organs of diabetic complications (Fig. 1). We used a novel real-time PCR-based assay to confirm our previous finding. A maximum (10-fold) increase in ET-1 mRNA expression was seen in the retina in diabetes. Diabetes also caused a significant (4-fold) increase in mRNA expression in both kidney and heart. Interestingly, bosentan treatment lowered ET-1 mRNA expression in all organs examined.

Diabetes-induced increased FN synthesis is blocked by ET antagonism. We have previously demonstrated (8, 12, 15) that hyperhexosemia-induced increased ET expression is an important mediator of increased ECM production in diabetes. One of the most important ECM proteins overexpressed in these organs due to diabetes is FN (15, 36). In the present study, we used a real-time PCR method to quantify FN mRNA expression. The primers used for FN RT-PCR were designed to allow assessment of total FN, including all splice variants of FN, in accordance with the guidelines for primer design for LightCycler. In all three target organs of diabetic complications, we found significantly increased FN mRNA expression in the poorly controlled diabetic animals compared with the age- and sex- matched nondiabetic rats (Fig. 2). Treatment of poorly controlled diabetic animals with a dual ET_A and ET_B antagonist completely prevented diabetes-induced increased FN mRNA expression in both retina and kidney. A partial prevention was noted in the heart, where bosentan-treated diabetic animal mRNA levels were not significantly different from either poorly controlled diabetic or nondiabetic rats (Fig. 2).

NF-κB activation in diabetes and modulation by ET antagonism. As we have previously reported (10), high glucose and ETs cause a time-dependent activation of NF-κB in endothelial cells. In the present study, we have demonstrated that a similar activation of NF-κB occurs in the target organs of diabetic complications (Fig. 3). The specificity of NF-κB activation was established by the supershift assay and the incubation with 100-fold unlabeled oligonucleotides (Fig. 3). However, there were variations in the level of activation. In parallel with ET-1 expression, the most pronounced activation was seen in the retina of diabetic animals

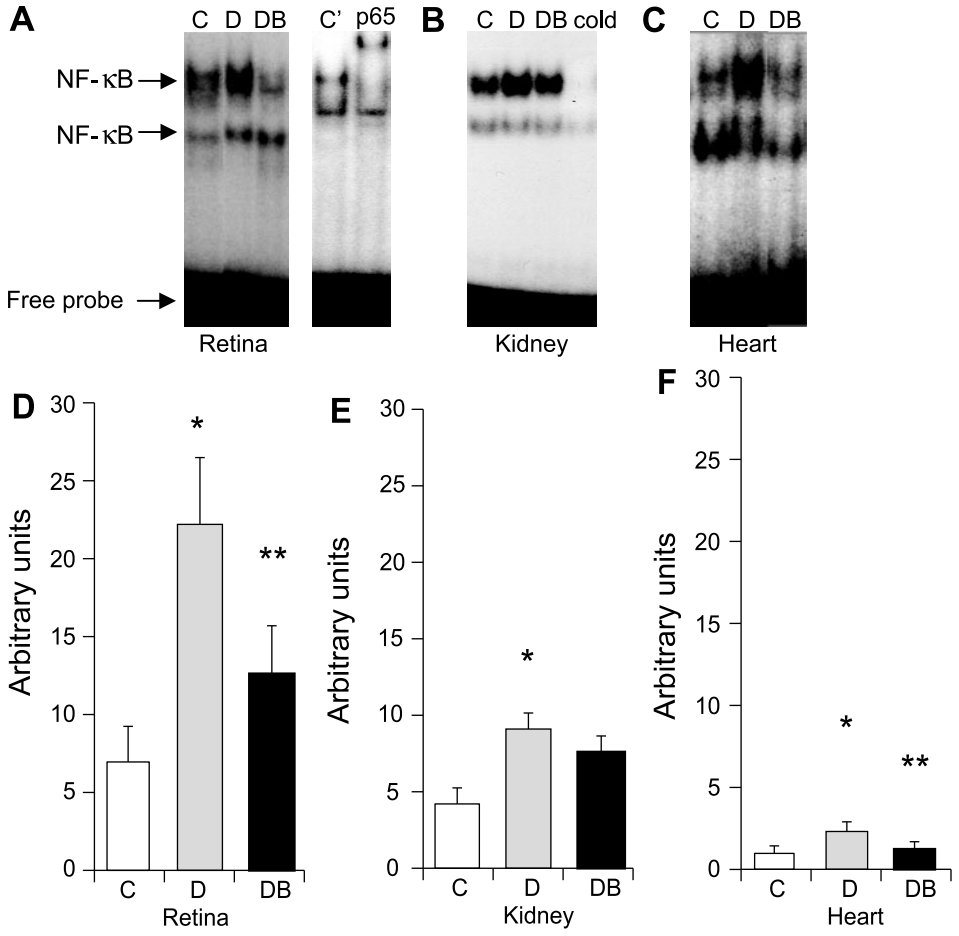

Fig. 3. Effects of diabetes on NF-κB activation in the retina (*A*), kidney (*B*), and heart (*C*) of the nondiabetic controls (C), poorly controlled diabetics (D), and bosentan-treated diabetics (DB) are shown in representative EMSA autoradiograms. In the retina, specificity is also being demonstrated by a representative supershift assay (p65) of a control sample (C′). Incubation with unlabeled oligonucleotide resulted in disappearance of the band, as demonstrated in a representative sample in the kidney (cold). *D–F*: semiquantitative analyses of respective autoradiograms. *Significantly different from C, **significantly different from D; $n = 6$ in each group, Although all samples were quantified after overnight exposure, the demonstrated autoradiograms of the heart (*C*) represent 3 days of exposure to enhance the bands.

(4-fold compared with nondiabetic animals, $P < 0.01$; Fig. 3). The arbitrary densitometric units, although increased (2-fold, $P < 0.05$) in the kidney of diabetic rats compared with the controls, were approximately one-half the retinal levels in diabetics. The lowest level (one-tenth of the retina in diabetes) of activation values were seen in the heart. However, poorly controlled diabetic animals still showed a higher level than the nondiabetic rats ($P < 0.05$). Diabetes-induced NF-κB activation was prevented by bosentan treatment in both the retina and heart but not the kidney (Fig. 3).

AP-1 activation in diabetes and modulation by ET antagonism. Transcription factor AP-1 also showed diabetes-induced activation. The specificity of AP-1 activation was further established by incubation with 100-fold unlabeled oligonucleotides (Fig. 4). However, there were variations in the level of activation. The most pronounced activation was seen in the retina of diabetic animals (6-fold compared with nondiabetic animals, $P < 0.01$; Fig. 4). The arbitrary densitometric units, although significantly increased (2-fold, $P < 0.05$) in both the kidney and heart of diabetic rats compared with the controls, were much lower compared with the retinal levels in diabetics. Diabetes-induced AP-1 activation was prevented by bosentan treatment in both the retina and kidney but not the heart (Fig. 4).

DISCUSSION

The key findings of the present study are that diabetes causes FN upregulation in the retina, kidney, and heart, the three organs involved in chronic diabetic complications. Diabetes-induced, increased tissue FN mRNA expression requires activation of both NF-κB and AP-1, at least in part, by an ET-mediated pathway, although the level of activation varies from organ to organ. ET receptor antagonism prevents FN mRNA expression in all three organs examined. However, the effects on transcription factor activation were variable among organs. In the retina, both NF-κB and AP-1 were important, whereas NF-κB activation appeared to be the predominant mechanism of diabetes-induced, ET-mediated FN synthesis in the heart. Similarly, AP-1 was the predominant mechanism in the kidney. Therefore, this study has demonstrated that, in diabetes, activation of transcription factors may be modulated by the tissue microenvironment.

Oxidative stress could be an important mechanism in the pathogenesis of diabetic complications (2). NF-κB and AP-1 can be activated by oxidative stress (1, 11, 38). Previous studies have demonstrated NF-κB activation in retinal capillary pericytes exposed to high glucose levels as well as retinal tissues in short-term diabetes (20, 34). Similarly, mesangial cells and renal

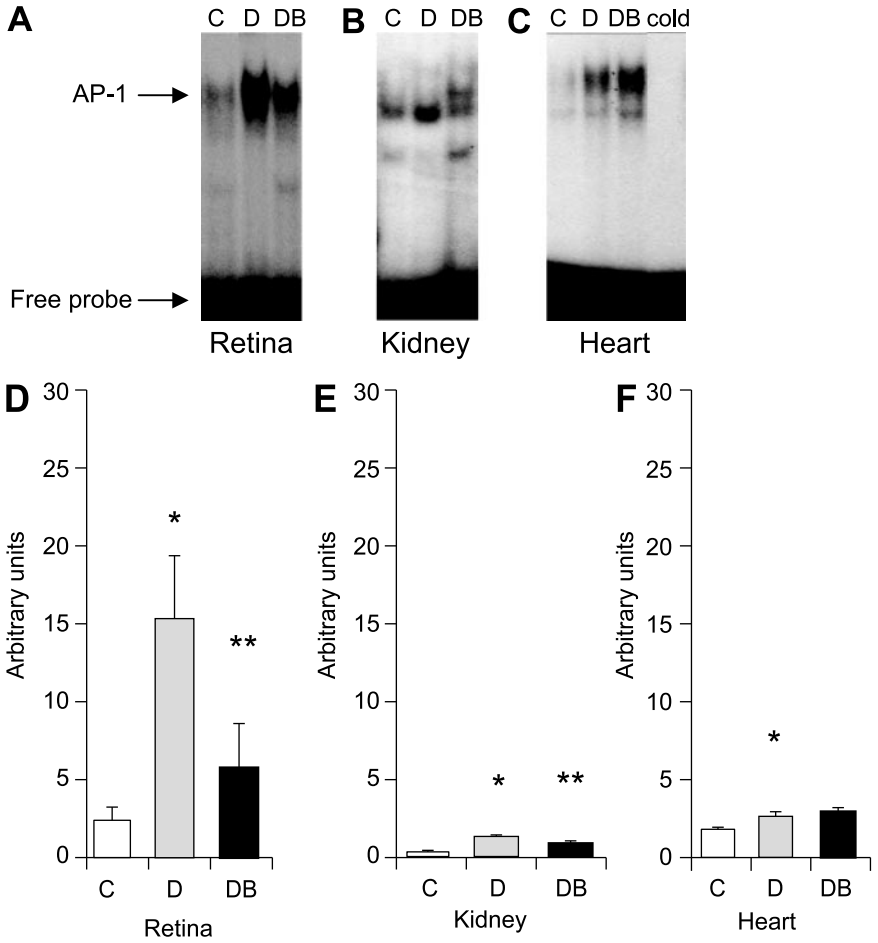

Fig. 4. Effects of diabetes on activating protein (AP)-1 activation in the retina (*A*), kidney (*B*), and heart (*C*) of nondiabetic controls (C), poorly controlled diabetics (D), and bosentan-treated diabetics (DB) are shown in representative EMSA autoradiograms. Incubation with unlabeled oligonucleotide resulted in disappearance of the band, as demonstrated in a representative sample in the heart (cold). *D–F*: semiquantitative analyses of respective autoradiograms. *Significantly different from C, **significantly different from D; $n = 6$ in each group. Although all samples were quantified after overnight exposure, the demonstrated autoradiograms of the heart (*C*) represent 3 days of exposure to enhance the bands.

tubular epithelial cells exposed to high glucose show NF-κB activation (19, 23, 24). In the hearts of rats, short-term diabetes demonstrated both NF-κB and AP-1 activation (32). This study has demonstrated that NF-κB and AP-1 are differentially activated in various target organs of diabetic complications after long-term diabetes. Furthermore, we have identified the effect of such activation in the pathogenesis of a characteristic lesion in diabetes. It is interesting to note that transcription factor activation exhibited variable patterns and levels in different tissues. The strongest activation of NF-κB and AP-1 was seen in the retina in diabetes, which also correlated with the highest ET-1 mRNA levels. The exact reasons for differential transcription factor activation are not clear. It appears that the tissue microenvironment may affect the activation of transcription factors in diabetes. However, the findings in this study may, in part, be helpful to explain the variation seen in BM thickening in different target organs (14). Blockade of NF-κB and AP-1 activation and augmented FN mRNA expression in diabetes by bosentan indicate the important role ETs play with respect to transcription factor activation leading to FN gene expression in diabetes.

We have previously demonstrated with endothelial cells how glucose-induced, ET-mediated increased FN synthesis is dependent on coordinated activation of both NF-κB and AP-1 (10). Several studies have demonstrated the effects of these transcription factors on FN synthesis. In hepatoma cells, NF-κB was shown to play both positive and negative regulator roles acting on the FN gene (25). Although several potential NF-κB-binding sites have been identified in the FN promoter, the functional significance of only a few has been determined. The regulation of FN gene expression has been shown to be offered by the −41 NF-κB-binding site (25). The DNA sequence between +1 and +136 has been determined for partial PKC-mediated activation of the FN gene in hepatoma cells (25). A potential NF-κB p65 response element present in the FN promoter may serve as a positive regulator of FN gene expression (25). Identification and characterization of an NF-κB-binding site in the promoter region of the FN gene responsible for ET responsiveness in endothelial cells require further investigation. An AP-1-binding site mediating angiotensin II-induced transcriptional activation of the FN gene has been shown in the promoter region (40). Whether ET-induced activation of the FN gene also utilizes the same region of the gene promoter remains to be investigated.

Furthermore, it is well known that hyperglycemia resulting from diabetes activates PKC (2, 18, 21). Activation of PKC is required for glucose-induced upregulation of ET in many cells, including endothelial cells (9, 27). Therefore, glucose causing an upregulation of ET expression through PKC activation can further activate transcription factors NF-κB and AP-1 and thereby increase FN expression. However, hyperhexosemia-induced ET upregulation can also be controlled by NF-κB and AP-1 (26, 27, 33). Furthermore, because ET receptors are predominantly G_q coupled, their activation may lead to activation of phospholipase C, elevation of intracellular Ca^{2+} concentration, and activation of PKC. Therefore, combining the results of our present study with the previously published studies (7, 26, 27, 33), we can speculate that PKC, NF-κB, and AP-1 can control both upstream and downstream effector molecules in the high glucose-induced signaling pathway. However, the role of ET receptor-mediated signaling in diabetes leading to NF-κB activation may potentially be influenced by other factors (31), which remain to be investigated.

In conclusion, we have demonstrated in three different organs that diabetes-induced FN upregulation involves variable activation of NF-κB and AP-1 transcription factors via an ET-mediated pathway. The observations made in the present study are likely to have relevance for vasculopathy in diabetes.

These studies were supported in part by grants from the Canadian Diabetes Association, in honor of Margaret Francis, and the Canadian Institute of Health Research (MOP 43841).

REFERENCES

1. **Bowie A and O'Neill LA.** Oxidative stress and nuclear factor-kappaB activation: a reassessment of the evidence in the light of recent discoveries. *Biochem Pharmacol* 59: 13–23, 2000.
2. **Brownlee M.** Biochemistry and molecular cell biology of diabetic complications. *Nature* 414: 813–820, 2001.
3. **Cagliero E, Roth T, Roy S, Maiello M, and Lorenzi M.** Expression of genes related to the extracellular matrix in human endothelial cells. Differential modulation by elevated glucose concentrations, phorbol esters, and cAMP. *J Biol Chem* 266: 14244–14250, 1991.
4. **Chakrabarti S, Cukiernik M, Hileeto D, Evans T, and Chen S.** Role of vasoactive factors in the pathogenesis of early changes in diabetic retinopathy. *Diabetes Metab Res Rev* 16: 393–407, 2000.
5. **Chakrabarti S and Sima AA.** Effect of aldose reductase inhibition and insulin treatment on retinal capillary basement membrane thickening in BB rats. *Diabetes* 38: 1181–1186, 1989.
6. **Chen F, Castranova V, and Shi X.** New insights into the role of nuclear factor-kappaB in cell growth regulation. *Am J Pathol* 159: 387–397, 2001.
7. **Chen S, Apostolova MD, Cherian MG, and Chakrabarti S.** Interaction of endothelin-1 with vasoactive factors in mediating glucose-induced increased permeability in endothelial cells. *Lab Invest* 80: 1311–1321, 2000.
8. **Chen S, Evans T, Deng D, Cukiernik M, and Chakrabarti S.** Hyperhexosemia induced functional and structural changes in the kidneys: role of endothelins. *Nephron* 90: 86–94, 2002.
9. **Chen S, Evans T, Mukherjee K, Karmazyn M, and Chakrabarti S.** Diabetes-induced myocardial structural changes: role of endothelin-1 and its receptors. *J Mol Cell Cardiol* 32: 1621–1629, 2000.
10. **Chen S, Mukherjee S, Chakraborty C, and Chakrabarti S.** High glucose-induced, endothelin-dependent, extracellular matrix protein synthesis is mediated via nuclear factor-κB and AP-1. *Am J Physiol Cell Physiol* 284: C263–C272, 2003.
11. **Chinenov Y and Kerppola TK.** Close encounters of many kinds: Fos-Jun interactions that mediate transcription regulatory specificity. *Oncogene* 20: 2438–2452, 2001.
12. **Deng D, Evans T, Mukherjee K, Downey D, and Chakrabarti S.** Diabetes-induced vascular dysfunction in the retina: role of endothelins. *Diabetologia* 42: 1228–1234, 1999.
13. **Dignam JD, Lebovitz RM, and Roeder RG.** Accurate transcription initiation by RNA polymerase II in a soluble extract from isolated mammalian nuclei. *Nucleic Acids Res* 11: 1475–1489, 1983.
14. **Engerman RL, Kern TS, and Garment MB.** Capillary basement membrane in retina, kidney, and muscle of diabetic dogs

and galactosemic dogs and its response to 5 years aldose reductase inhibition. *J Diabetes Complications* 7: 241–245, 1993.
15. **Evans T, Deng DX, Chen S, and Chakrabarti S.** Endothelin receptor blockade prevents augmented extracellular matrix component mRNA expression and capillary basement membrane thickening in the retina of diabetic and galactose-fed rats. *Diabetes* 49: 662–666, 2000.
16. **Gallois C, Habib A, Tao J, Moulin S, Maclouf J, Mallat A, and Lotersztajn S.** Role of NF-kappaB in the antiproliferative effect of endothelin-1 and tumor necrosis factor-alpha in human hepatic stellate cells. Involvement of cyclooxygenase-2. *J Biol Chem* 273: 23183–23190, 1998.
17. **Henkel T, Machleidt T, Alkalay I, Kronke M, Ben Neriah Y, and Baeuerle PA.** Rapid proteolysis of I kappa B-alpha is necessary for activation of transcription factor NF-kappa B. *Nature* 365: 182–185, 1993.
18. **Ishii H, Koya D, and King GL.** Protein kinase C activation and its role in the development of vascular complications in diabetes mellitus. *J Mol Med* 76: 21–31, 1998.
19. **Jones S, Jones S, and Phillips AO.** Regulation of renal proximal tubular epithelial cell hyaluronan generation: implications for diabetic nephropathy. *Kidney Int* 59: 1739–1749, 2001.
20. **Joussen AM, Poulaki V, Mitsiades N, Kirchhof B, Koizumi K, Dohmen S, and Adamis AP.** Nonsteroidal anti-inflammatory drugs prevent early diabetic retinopathy via TNF-alpha suppression. *FASEB J* 16: 438–440, 2002.
21. **King GL and Brownlee M.** The cellular and molecular mechanisms of diabetic complications. *Endocrinol Metab Clin North Am* 25: 255–270, 1996.
22. **Kornblihtt AR, Umezawa K, Vibe-Pedersen K, and Baralle FE.** Primary structure of human fibronectin: differential splicing may generate at least 10 polypeptides from a single gene. *EMBO J* 4: 1755–1759, 1985.
23. **Kumar A, Hawkins KS, Hannan MA, and Ganz MB.** Activation of PKC-βI in glomerular mesangial cells is associated with specific NF-κB subunit translocation. *Am J Physiol Renal Physiol* 281: F613–F619, 2001.
24. **Lal MA, Brismar H, Eklof AC, and Aperia A.** Role of oxidative stress in advanced glycation end product-induced mesangial cell activation. *Kidney Int* 61: 2006–2014, 2002.
25. **Lee BH, Kim MS, Rhew JH, Park RW, de Crombrugghe B, and Kim IS.** Transcriptional regulation of fibronectin gene by phorbol myristate acetate in hepatoma cells: a negative role for NF-kappaB. *J Cell Biochem* 76: 437–451, 2000.
26. **Levin ER.** Endothelins. *N Engl J Med* 333: 356–363, 1995.
27. **Levin ER.** Endothelins as cardiovascular peptides. *Am J Nephrol* 16: 246–251, 1996.
28. **Madri JA, Pratt BM, and Yannariello-Brown J.** Matrix-driven cell size change modulates aortic endothelial cell proliferation and sheet migration. *Am J Pathol* 132: 18–27, 1988.
29. **Mizutani M, Kern TS, and Lorenzi M.** Accelerated death of retinal microvascular cells in human and experimental diabetic retinopathy. *J Clin Invest* 97: 2883–2890, 1996.
30. **Mohamed AK, Bierhaus A, Schiekofer S, Tritschler H, Ziegler R, and Nawroth PP.** The role of oxidative stress and NF-kappaB activation in late diabetic complications. *Biofactors* 10: 157–167, 1999.
31. **Muller DN, Mullally A, Dechend R, Park JK, Fiebeler A, Pilz B, Loffler BM, Blum-Kaelin D, Masur S, Dehmlow H, Aebi JD, Haller H, and Luft FC.** Endothelin-converting enzyme inhibition ameliorates angiotensin II-induced cardiac damage. *Hypertension* 40: 840–846, 2002.
32. **Nishio Y, Kashiwagi A, Taki H, Shinozaki K, Maeno Y, Kojima H, Maegawa H, Haneda M, Hidaka H, Yasuda H, Horiike K, and Kikkawa R.** Altered activities of transcription factors and their related gene expression in cardiac tissues of diabetic rats. *Diabetes* 47: 1318–1325, 1998.
33. **Quehenberger P, Bierhaus A, Fasching P, Muellner C, Klevesath M, Hong M, Stier G, Sattler M, Schleicher E, Speiser W, and Nawroth PP.** Endothelin 1 transcription is controlled by nuclear factor-kappaB in AGE-stimulated cultured endothelial cells. *Diabetes* 49: 1561–1570, 2000.
34. **Romeo G, Liu WH, Asnaghi V, Kern TS, and Lorenzi M.** Activation of nuclear factor-kappaB induced by diabetes and high glucose regulates a proapoptotic program in retinal pericytes. *Diabetes* 51: 2241–2248, 2002.
35. **Roux S, Breu V, Ertel SI, and Clozel M.** Endothelin antagonism with bosentan: a review of potential applications. *J Mol Med* 77: 364–376, 1999.
36. **Roy S, Cagliero E, and Lorenzi M.** Fibronectin overexpression in retinal microvessels of patients with diabetes. *Invest Ophthalmol Vis Sci* 37: 258–266, 1996.
37. **Schreiber E, Matthias P, Muller MM, and Schaffner W.** Rapid detection of octamer binding proteins with "mini-extracts," prepared from a small number of cells. *Nucleic Acids Res* 17: 6419, 1989.
38. **Shaulian E and Karin M.** AP-1 in cell proliferation and survival. *Oncogene* 20: 2390–2400, 2001.
39. **Shono T, Ono M, Izumi H, Jimi SI, Matsushima K, Okamoto T, Kohno K, and Kuwano M.** Involvement of the transcription factor NF-kappaB in tubular morphogenesis of human microvascular endothelial cells by oxidative stress. *Mol Cell Biol* 16: 4231–4239, 1996.
40. **Tamura K, Nyui N, Tamura N, Fujita T, Kihara M, Toya Y, Takasaki I, Takagi N, Ishii M, Oda K, Horiuchi M, and Umemura S.** Mechanism of angiotensin II-mediated regulation of fibronectin gene in rat vascular smooth muscle cells. *J Biol Chem* 273: 26487–26496, 1998.
41. **Yamada KM.** Cell surface interactions with extracellular materials. *Annu Rev Biochem* 52: 761–799, 1983.